Pseudogene OCT4-pg5 Upregulates OCT4B Expression to Promote Bladder Cancer Progression by Competing with miR-145-5p

Wuer Zhou
General Hospital of Southern Theatre Command, PLA
Yue Yang
General Hospital of Southern Theatre Command, PLA
Wei Wang (wangweiccc@hotmail.com)
General Hospital of Southern Theatre Command, PLA
Chenglin Yang
General Hospital of Southern Theatre Command, PLA
Zhi Cao
General Hospital of Southern Theatre Command, PLA
Xiaoyu Lin
General Hospital of Southern Theatre Command, PLA
Huifen Zhang
General Hospital of Southern Theatre Command, PLA
Yuansong Xiao
General Hospital of Southern Theatre Command, PLA
Xiaoming Zhang
General Hospital of Southern Theatre Command, PLA

Research Article

Keywords: OCT4-pg5, OCT4B, miR-145-5p, competing endogenous RNA, bladder cancer

Posted Date: April 19th, 2022

DOI: https://doi.org/10.21203/rs.3.rs-1528804/v1

Abstract

Background

Bladder cancer (BC) is one of the most common malignant neoplasms worldwide, and is characterized by metastasis and insensitivity to chemotherapy. We aim to construct competing endogenous RNA (ceRNA) networks to identify potential progression and prognostic markers associated with BC.

Methods

We first extracted the expression profiles of RNAs from The Cancer Genome Atlas (TCGA) database and used bioinformatic analysis to establish ceRNAs in BC. Real-time quantity PCR (RT-qPCR) was performed to measure OCT4-pg5 and OCT4B expressions in different bladder cell lines and different grades of cancer. The effects of OCT4-pg5, OCT4B and miR-145-5p on proliferation and metastasis were determined by in vitro and in vivo experiments. Luciferase reporter assay was carried out to reveal the interaction among OCT4-pg5, OCT4B and miR-145-5p. Flow cytometry was performed to explore the effects of OCT4-pg5 and OCT4B expression on the cell cycle phases distribution of T24 cells.

Results

The OCT4-pg5/miR-145-5p/OCT4B ceRNA network was related to the progression and prognosis of BC. OCT4-pg5 expression was significantly increased in BC cell lines, which was correlated with OCT4B expression and advanced tumor grade. Overexpression of OCT4-pg5 and OCT4B promoted the proliferation and invasion of BC cells, while miR-145-5p suppressed these activities. Mechanically, OCT4-pg5 3’ untranslated region (3’UTR) competed for miR-145-5p, thereby increasing OCT4B expression. In addition, OCT4-pg5 promoted EMT by activating the Wnt/β-catenin pathway and upregulating the expression levels of matrix metalloproteinases (MMPs) 2 and 9 as well as transcription factors zinc finger E-box binding homeobox (ZEB) 1 and 2. Furthermore, elevated expression of OCT4-pg5 and OCT4B reduced the sensitivity of BC cells to cisplatin by reducing apoptosis and increasing the proportion of cells in G1.

Conclusions

These findings indicate that OCT4-pg5/miR-145-5p/OCT4B axis promotes the progression of BC by inducing EMT via Wnt/β-catenin pathway and enhances the cisplatin resistance. It could be prospect for the therapeutic approaches for BC.

Background

Bladder cancer (BC) is one of the most common urological malignant neoplasms, with approximately 570,000 new cases diagnosed in 2020 (1). Incidence and mortality of BC are positively correlated with smoking and Gross Domestic Product (GDP) per capita (2), so incidence is expected to continue rising in developing countries. Moreover, BC is characterized by high rates of recurrence, metastasis, and insensitivity to chemotherapy (3). Consequently, it is critical to elucidate the molecular pathogenesis of BC to identify more efficacious treatment targets.

Octamer-binding transcription factor 4 (OCT4), one of the POU domain-containing family of transcription factors, is implicated in the pathogenesis of multiple cancer types. The OCT4 gene can generate at least three distinct mRNA transcripts and proteins by alternative splicing and alternative translation initiation (4, 5). In recent years, there has been increasing interest in OCT4B, which cannot sustain ES cell self-renewal but may respond to cell stress (6–8). Hypoxia stimulates a short OCT4 isoform, OCT4B, via a hypoxia inducible factor (HIF) 2α-dependent pathway to induce epithelial–mesenchymal transition (EMT) and facilitate cancer dissemination (9–11). Further, OCT4B is highly expressed in BC and glioblastoma cells, and expression is correlated with poorer histopathological grade and clinical prognosis (12, 13), but its pathogenic function in BC is still unknown.

MicroRNA-145 (miR-145) functions as a tumor-suppressor in multiple cancers, including non-small-cell lung, bladder, and colorectal cancer, by downregulating its oncogenes (14, 15). In addition, miR-145 can bind directly to the 3’untranslated region (3’UTR) of OCT4 mRNA, thereby inhibiting the proliferation, infiltration, and migration of prostate cancer (16), while the relationship between miR-145-5p and OCT4B/OCT4-pg5 is still lack of reports in BC.

Long non-coding RNAs (lncRNAs), defined as untranslated RNA transcripts longer than 200 nucleotides, are now recognized as important regulators of tumorigenesis and progression (17), and are considered potential biomarkers for the early detection, diagnosis, and prognosis of BC (18). Pseudogenes are non-functional copies of genes that also produce lncRNAs (19), and it is now recognized that pseudogene lncRNAs can regulate tumor progression, mainly by competing with miRNAs for binding to parent genes and thereby interfering with miRNA-mediated gene suppression (20). For instance, OCT4-pg5 is an OCT4 pseudogene typically transcribed in cancer tissues that may upregulate OCT4 expression by acting as an ‘RNA sponge’ to prevent inhibition by miR-145 (21, 22). However, the functions of OCT4-pg5, OCT4B, and miR-145-5p in BC have not been established.

In this study, we report that OCT4-pg5 expression is elevated in BC cells and tissues concomitantly with OCT4B, and that higher expressions of OCT4-pg5 and OCT4B are strongly associated with more advanced pathological grade and stage. Subsequent functional studies including cell viability, cell migration, and Luciferase-based gene expression assays further indicated that OCT4-pg5 acts as a competing endogenous RNA (ceRNA) promoting OCT4B expression by sponging miR-145-5p, thereby interfering with miR-145-5p-mediated OCT4B downregulation and increasing BC cell metastatic capacity and drug resistance.

Methods

Data preparation and processing

We downloaded primitive data (expressing profiles) and clinic information of human Bladder Urothelial Carcinoma (BLCA) from TCGA database (https://portal.gdc.cancer.gov/). Available mRNA sequencing (mRNA-seq) data and miRNA sequencing (miRNA-seq) data from 408 BLCA samples were gained from TCGA database. All raw RNA-seq data (miRNAs and mRNAs) were normalized as fragments per kilobase of exon model per million mapped fragment reads. Transformation of miRNA sequences into human mature miRNA names was accomplished using the miRBase database (https://www.mirbase.org/).

Screening of differentially expressed RNAs (DERNAs)

When performing the differential expression analysis in $OCT4B^{high}$ and $OCT4B^{low}$ BLCA samples, we determined the DERNAs (including lncRNAs, miRNAs, and mRNAs) with thresholds of |logFC| >2 and p <0.05. Volcano plots of the DERNAs [including differentially expressed lncRNAs (DElncRNAs), differentially expressed miRNAs (DEmiRNAs), and differentially expressed mRNAs (DEmRNAs)] were visualized using R language (version 4.1.2).

Establishment of the ceRNA network in BC

The ceRNA network was constructed by the following steps: (1) StarBase (http://starbase.sysu.edu.cn/) and TargetScan (version 7.2, http://www.targetscan.org/) was used to predict the DEmiRNAs and DEmRNAs, and build the miRNA-mRNA interaction pairs; (2) StarBase database was used to forecast the DEmiRNAs and DElncRNAs, and build the lncRNA-miRNA interaction pairs; (3) the VennDiagram package in R software was utilized to compare the target genes with DEmRNAs, and the target genes that overlapped with DEmRNAs in this study were selected for the next analysis to build the lncRNA-miRNA-mRNA triple regulatory network.

The Cytoscape plug-in cytoHubba was performed to identify the hub lncRNA-miRNA-mRNA triple regulatory network. The generated networks were visualized by Cytoscape software (version 3.7.0, https://www.cytoscape.org/).

Functional enrichment analysis

For the sake of understanding the possible biological processes and pathways of the network, we firstly conducted a functional enrichment analysis of the DERNAs in the lncRNA-miRNA-mRNA triple regulatory network in Metascape (http://metascape.org/gp/index.html). Then, GO enrichment (including BP, CC, and MF) and KEGG pathway analyses of these RNAs were performed using Metascape.

Survival analysis and construction of a specific prognosis model for BC

The survival status and time of BLCA patients were gained from TCGA clinical dataset. We used R software to perform Kaplan-Meier analysis and a log-rank test to determine the relationship between the OCT4-pg5/miR-145-5p/OCT4B ceRNA network with the overall survival (OS) of BLCA patients in TCGA database.

Cell culture and clinical samples

Five human bladder cancer cell lines (T24, 5637, and TCCSUP were from American Type Culture Collection (ATCC, Manassas, VA, USA), EJ was obtained from Japanese Cancer Research Resources Bank (JCRB, Tokyo, Japan), and the BIU-87 bladder cancer cell line from China Center for Type Culture Collection (CCTCC, Wuhan, China)), and an immortalized human bladder epithelial cell line (SV-HUC-1 was from ATCC) were preserved in RPMI 1640 (Gibco, Grand Island, NY) or DMEM (Gibco) supplemented with 10% fetal bovine serum (FBS; Gibco) in an atmosphere of 5% CO_2 at 37 °C. These cell lines were authenticated by short tandem-repeat (STR) profiling, and within 4 passages from purchase.

A total of 140 human bladder cancer tissue samples and 34 adjacent bladder epithelial tissue samples were obtained from the General Hospital of Southern Theater Command (China) from February 2016 to October 2019. Inclusion criteria were confirmed non-muscle-invasive bladder cancer (NMIBC, n=70) or muscle-invasive bladder cancer (MIBC, n=70), while the exclusion criterion was metastasis before surgery. All patients provided informed written consent, and the study was approved by the Institute Research Ethics Committee, General Hospital of Southern Theater Command, China, and followed the guidance of Declaration of Helsinki.

Plasmid construction and transfection

Human miR-145-5p mimics and its negative controls (NC mimics), miR-145-5p inhibitors and its negative controls (NC inhibitors) were acquired from Vipotion Biotechnology (Guangzhou, China). Besides, OCT4-pg5 (NR_131184.1), OCT4B (NM_203289.6, ENSG00000236375), OCT4-pg5 siRNAs (si-OCT4-pg5), OCT4B siRNAs (si-OCT4B), miR-145-5p mimics (miR-145), OCT4-pg5 plus miR-145-5p mimics (OCT4-pg5+miR-145-5p), and empty pcDNA3.1(+) (control) were all from Vipotion Biotechnology. Moreover, these PCR products were digested with BamHI//NotI and cloned into the vectors, followed by DNA sequence verification. T24 or 5637 cells were separately transfected with these plasmids using Lipofectamine 2000 reagent (Invitrogen, Carlsbad, CA) for 48h according to the manufacturer’s protocol.

RNA extraction and real-time PCR analysis

Total RNA was extracted from tissues or cells using TRIZOL reagent (Invitrogen Life Technologies) according to the manufacturer's instructions. Real-time PCR was performed using a Stratagene Mx3000P Real-time PCR System (Applied Biosystems, Agilent Stratagene, America) and Bestar qPCR RT Kit (DBI Bioscience, Shanghai, China). The amplification procedure was as follows: 94 °C for 2 min, followed by 40 cycles of 94 °C for 20 s, 58 °C for 20 s, and 72 °C for 20 s. A dissociation step was performed to generate a melting curve for confirmation of amplification specificity. For miR-145-5p, U6 was used as the

internal reference, while GAPDH was used as the reference for others. Relative gene expression levels were calculated using the $2^{-\Delta\Delta Ct}$ method. All primers used were designed and produced by Vipotion Biotechnology, and are listed in Table S6.

Luciferase reporter assay

The wild-type 3'UTR sequence of OCT4B containing the putative miR-145-5p binding site was cloned into psiCHECK2 (Promega, Madison, WI, USA) to construct a 3'UTR luciferase reporter. For miRNA target analysis, cell lines (T24 and 5637) were transfected with the luciferase reporter and co-transfected with empty vector (control), miR-145-5p, wild-type OCT4-pg5 (wt-OCT4-pg5), wild-type OCT4-pg5 plus miR-145-5p or empty (control), miR-145-5p, mut-type OCT4-pg5 (mut-OCT4-pg5), or mutant-type OCT4-pg5 plus miR-145-5p plasmid as indicated. The luciferase activities were measured 48 h after transfection using a Dual-Luciferase Reporter Assay Kit (Promega) according to the manufacturer's instructions.

Immunofluorescence staining

After transfection, T24 or 5637 cells were grown on glass chamber slides to 90% confluence, fixed with 4% paraformaldehyde for 20 min, permeabilized with 0.1% Triton X-100 in phosphate-buffered saline (PBS) for 30 min, and blocked with 3% bovine serum albumin (BSA) in PBS for 1h at room temperature. Cells were then incubated with anti-OCT4B, anti-β-catenin, anti-E-cadherin, and anti-vimentin antibodies overnight at 4 °C. Immunolabeled cells were incubated with FITC-conjugated secondary antibody (Bioworld, Atlanta, GA, USA) for 1 h and finally counterstained with DAPI for 15 min. Staining patterns were examined and captured using a laser scanning confocal microscope.

Western blotting

Total cellular protein was extracted in lysis buffer (Beyotime; Shanghai, China) and quantified using the Bradford method. Proteins were separated by 10% sodium dodecyl sulfate-polyacrylamide gel electrophoresis (SDS-PAGE) and transferred electrophoretically onto polyvinylidene difluoride membranes (Millipore, USA). The membranes were incubated overnight at 4 °C with the following primary antibodies: anti-OCT4B, anti-N-cadherin, anti-β-catenin (all from Santa Cruz Biotechnology; Dallas, TX, USA), anti-vimentin, anti-E-cadherin, and anti-GAPDH (all from Affbiotech; Shanghai, China). Protein levels were quantified by densitometry using Image-Pro Plus 6.0.

Cell viability assay

Cell proliferation was measured using the Cell Counting Kit-8 (Dojindo, Cat. No.CK04) according to the manufacturer's instructions. T24 or 5637 cells were seeded in 96-well culture plates at 1×10^4 cells/well, cultured overnight, transfected with the indicated plasmids for 48 h, washed, and cultivated in complete medium for the indicated growth period (0, 24, 48, and 72 h). Cells were then treated with 10 ml /well Cell Counting Kit-8 solution for 4 h, and total viable cell number estimated by the absorbance at 450 nm using a microplate reader (Thermo Fisher Scientific, Multiskan MK3).

Migration and invasion assays

In vitro migration and invasion assays were conducted using uncoated and Matrigel-coated 24-well transwell chambers (pore size of 8 μM; Costar, Corning, NY, USA), respectively, according to the manufacturer's instructions. T24 or 5637 cells were plated at 5×10^5/well in the upper chambers of 24-well transwell plates with FBS-free medium, while the bottom chambers were filled with culture medium containing 20% FBS. After 48 h of incubation at 37 °C in a humidified 5% CO_2 atmosphere, cells in the upper chambers were removed, and migratory or invasive cells were stained with 0.1% crystal violet solution for 15 min. Total cell numbers from 6 randomly chosen fields per membrane were quantified at 200× magnification. Mean cell numbers from triplicate assays were calculated for each condition.

Wound-healing assay

After transfection, T24 cells were seeded into 6-well plates at 2×10^5 cells/well and allowed to grow to 90% confluence in complete medium. Cell monolayers were then wounded using a sterile plastic pipette tip, washed three times with PBS to remove cell debris, and incubated in serum-free medium for 24 h. Cells migrating into the wound area were photographed under an inverted microscopy at designated times, and the average distance of migration was calculated.

Colony formation assays

Transfected T24 or 5637 cells were seeded in 6-well plates at 500 cells/well and cultured for 10 days. Colonies were fixed in paraformaldehyde, stained with crystal violet, photographed, and counted.

Cell cycle and apoptosis analyses

Cell cycle and apoptosis analyses were conducted by flow cytometry (FCM) using a FACS Calibur flow cytometer (BD Biosciences, San Jose, CA, USA). For cell cycle analysis, transfected cells were plated at 5×10^5/mL in 6-well plates, incubated for 4–6 h in complete medium, washed with PBS, and then incubated in fresh complete medium for another 48 h. Cells were harvested, centrifuged, and fixed in 70% cold ethanol for 2 h. DNA staining was conducted using 300 ml /well cell cycle staining kit solution (Vazyme Biotech, Nanjing, China) for at least 15 min under darkness. For cell apoptosis analysis, cells transfected as indicated were stained using an AnnexinV-FITC Apoptosis Detection Kit (Vazyme Biotech). The proportion of apoptotic cells was analyzed by FCM using Cell Quest software.

Xenograft tumor model

Six-week-old BALB/c nude mice were acquired from the Model Animal Research Center of Southern Medical University. All animal experiments approved by the Institutional Animal Care and Use Committee of the General Hospital of Southern Theater Command. To establish the xenograft tumor model, 5×10^6 T24 cells stably transfected with si-OCT4-pg5 or NC-si-RNA, and 5×10^6 5637 cells stably transfected with pcDNA3.1(+)/OCT4-pg5 or NC-pcDNA3.1(+) were injected subcutaneously in the left flank of separate

BALB/c nude mice groups. Tumor volumes were evaluated every three days and calculated according to the equation

$$V(mm^3) = \frac{A \times B^2}{2} \quad ,$$

where A is the largest diameter and B is the perpendicular diameter. After 27 days, mice were sacrificed and tumors were isolated and weighted.

Statistical analysis

All statistical analyses were performed using SPSS 22.0, and graphs were constructed using GraphPad Prism 5. Results are expressed as mean ± SD of at least three independent experiments. Group means were compared using independent samples *t*-test. Categorial data were analyzed by the chi-square test or Fisher exact test. $P < 0.05$ (two-tailed) was regarded as statistically significant for all tests.

Results

OCT4B expression is upregulated and associated with poor prognosis in bladder cancer (BC)

To investigate the possible role of OCT4B in BC, we found that OCT4B was overexpressed in BC, but down-expressed in normal in the TCGA database (**Fig. 1A**). Furthermore, 133 DElncRNA (55 upregulated and 78 down-regulated), 175 DEmiRNAs (154 upregulated and 21 down-regulated), and 250 DEmRNAs (68 upregulated and 182 down-regulated) were sorted out from BC samples (**Fig. 1B**), and we constructed potential ceRNA networks (**Fig. 1C**). Finally, we selected OCT4-pg5/miR-145-5p/ OCT4B as target for following study (**Fig. 1D**). To further explore the potential functions associated with the triple regulatory network, functional enrichment analysis (including GO and KEGG) showed that the differentially expressed RNAs (DERNAs) participating in the network were particularly enriched in the “NABA MATRISOME ASSOCIATED,” “Formation of the cornified envelope”, and “T cell activation” (**Fig. 1E**). Then, the overall survival (OS) analysis showed that the OS rate in high OCT4B and OCT4-pg5 expression groups was worse than of low expression groups, low miR-145-5p expression group was worse than of high expression group, indicating that the ceRNA network constructed in present study might be a novel prognostic factor for BLCA patients **(Fig. 1F)**.

To identify potential contributions of OCT4-pg5 to BC development and pathological grade, we found that expression of OCT4-pg5 was significantly higher in cancer tissues than adjacent normal tissue as measured by RT-PCR (**Fig. 1G**), and higher expression level was associated with advanced pathological grade (**Fig. 1H**), suggesting OCT4-pg5 as a potential prognostic marker. Moreover, OCT4-pg5 expression was strongly and positively correlated with OCT4B expression in BC tissues (**Fig. 1I**), suggesting possible co-regulation. Comparing mRNA expression levels between BC tissues and normal adjacent tissues, as well as between five BC cell lines (T24, EJ, 5637, BIU-87, and TCCSUP) and a normal bladder cell line (SV-

HUC-1), we found OCT4-pg5 expression was highest in T24 cells, and moderately upregulated in 5637 and EJ cells (**Fig. 1J,** the expression levels were normalized to GAPDH expression).

We further investigated if miR-145-5p and OCT4 isoforms (OCT4B and OCT4-pg5) expression levels detected by qRT-PCR were associated with pathological or clinical features. As shown in **Table S1-5,** low miR-145-5p and high OCT4 isoforms expression levels were significantly correlated with greater tumor clinical stage and pathological grade, but not with patient sex, age, or smoking history.

MicroRNA(miR)-145-5p repressed migration and invasion of BC in vitro

To evaluate the biological significance of miR-145-5p in BC, we transfected T24 and 5637 cells with vectors expressing miR-145-5p inhibitors or miR-145-5p mimics, and tested for changes in migration and invasive capacity. Wound-healing assays showed that miR-145-5p overexpression significantly reduced T24 and 5637 cell migrations, compared to the negative control (NC) groups, while miR-145-5p inhibitor significantly promoted the migration compared to NC inhibitor groups (**Fig. 2A,B**). Further, transwell assays showed that miR-145-5p downregulation significantly enhanced the number of cells migrating and invading from the top transwell chamber into untreated and Matrigel-coated membranes, while miR-145-5p overexpression reversed these effects (**Fig. 2C-F**).

OCT4-pg5 and OCT4B functioned as oncogenes in BC in vitro and in vivo

To evaluate the effects of OCT4-pg5 on the oncogenic properties of BC cells, we tested for changes in the proliferation and invasive capacities of high OCT4-pg5 expression T24 cells and low OCT4-pg5 expression 5637 cells both in vitro and in vivo. Transfection of T24 cells with si-OCT4-pg5 (knockdown group) significantly reduced both the proliferation rate and the number of cell colonies formed after 72 h compared to cultures transfected with control vector (**Fig. 3A-C**). Conversely, OCT4-pg5 transfection increased the proliferation and colony formation rates of 5637 cells **(Fig. 3B-D)**. In addition, OCT4-pg5 knockdown significantly weakened the invasive capacity of T24 cells in transwell assays, while the OCT4-pg5 transfection enhanced the invasive capacity of 5637 cells (**Fig. 3E,F**). Mice injected with OCT4-pg5 overexpressing 5637 cells developed significantly larger tumors than mice injected with untransfected cells, and injected with OCT4-pg5 knockdown T24 cells significantly decreased tumors volume compared to control group (**Fig. 3G-I**). Moreover, overexpression of miR-145-5p partially inhibited the enhanced proliferation, colony formation and invasion of 5637 cells induced by OCT4-pg5 overexpression (**Fig. 3B,D,F**). On the contrary, OCT4-pg5 overexpression partly reversed the suppression caused by miR-145-5p (**Fig. 3B,D,F**). These results suggest that OCT4-pg5 functions by altering the activity of miR-145-5p.

The same assays were conducted to assess the oncogenic functions of OCT4B. Knockdown of OCT4B significantly inhibited proliferation, while overexpression increased BC cell invasiveness in transwell assays (**Fig. 3A,C,E**), suggesting that OCT4B may promote cancer progression.

The OCT4-pg5 upregulated OCT4B expression by sequestering miR-145-5p

The prediction of the secondary structures after miR-145-5p binding using RNAhybrid (https://bibiserv.cebitec.uni-bielefeld.de/RNAhybrid) yielded identical free energy changes (-28.9 kcal/mol) for the OCT4-pg5 3'UTR (3'UTR of OCT4-pg5 corresponds to 300 bases downstream of the nucleotide sequence) and OCT4B 3'UTR (**Fig. 4A,B, Fig. S1**), indicating that OCT4-pg5 and OCT4B have a similar affinity for miR-145-5p. Moreover, luciferase assays showed that overexpression of wt-OCT4-pg5 in T24 and 5637 cells significantly increased the activity of wild-type OCT4B 3'UTR reporter, while inhibition of OCT4B by miR-145-5p was reversed upon transfection with wt-OCT4-pg5 (**Fig. 4C**). However, these effects were not found following mut-OCT4-pg5 transfection (**Fig. 4D**). Collectively, these results suggest that OCT4-pg5 3'UTR may compete with miR-145-5p for OCT4B 3'UTR binding in BC, thereby allowing OCT4B upregulation.

To verify these results, we conducted qRT-PCR and western blot of lysates from transfected T24 and 5637 BC cells and found that overexpression of miR-145-5p significantly downregulated both OCT4B (**Fig. 4E,F,K,L**) and OCT4-pg5 (**Fig. 4I,J**). Further, suppression of OCT4B expression in 5637 cells by miR-145-5p transfection could be partly abolished by transfection of OCT4-pg5 overexpression plasmid (**Fig. 4F,L**). In addition, OCT4-pg5 knockdown significantly decreased OCT4B mRNA and protein expression in T24 cells (**Fig. 4E,K**). Thus, the expression of miR-145-5p was upregulated when OCT4-pg5 was knockdown in T24 cells (**Fig. 4G)**, and downregulated when OCT4-pg5 transfected in 5637 cells (**Fig. 4H)**, while these results were not found in OCT4B (**Fig. 4G,H**). Immunofluorescence assays also revealed that OCT4B was located in the cytoplasm, and either OCT4-pg5 knockdown or miR-145-5p overexpression suppressed OCT4B expression (**Fig. 4M**). While the suppression of OCT4B expression in 5637 cells by miR-145-5p transfection could be reversed by transfection of OCT4-pg5 (**Fig. 4N**).

To further verify the effect of OCT4-pg5 on BC cell in vivo, T24 and 5637 cells stably transduced with different vectors were subcutaneously injected into BALB/c nude mice. The results revealed that OCT4-pg5 and OCT4B overexpression promoted the growth of tumor, while miR-145-5p inhibited these effects, and OCT4-pg5 could abrogate the OCT4-pg5-induced inhibition in BC **(Fig. 4O,P**). These results indicated that OCT4-pg5 may upregulate OCT4B expression by sponging miR-145-5p.

OCT4-pg5 promoted metastasis by regulating epithelial-mesenchymal transition

Epithelial-mesenchymal transition (EMT) promotes cancer progression by enhancing invasive capacity. To examine if OCT4-pg5 regulates EMT in BC, we measured the expression levels of EMT-associated transcription factors in T24 and 5637 cells. Down-expression of OCT4-pg5 or OCT4B in T24 cells resulted in increased expression levels of E-cadherin (an epithelial marker) mRNA (**Fig. 5A**) and protein (**Fig. 5F**), and lower expression levels of N-cadherin, and vimentin (mesenchymal markers) mRNAs (**Fig. 5B-D**) and proteins (**Fig. 5F**). In contrast, the OCT4-pg5 or OCT4B transfected 5637 cells expressed low mRNA (**Fig. 5A**) and protein (**Fig. 5F**) levels of E-cadherin while high expression levels of N-cadherin, and vimentin mRNAs (**Fig. 5B-D**) and proteins (**Fig. 5F**). Further, T24 and 5637 cells stably transduced with different vectors were subcutaneously injected into BALB/c nude mice, and the EMT makers were detected from the tumor grew in the mice by Western blot. The results revealed that OCT4-pg5 and OCT4B

overexpression upregulated N-cadherin and vimentin, and down-expressed E-cadherin, while miR-145-5p inhibited these effects, and OCT4-pg5 could abrogate the OCT4-pg5-induced effects in BC **(Fig. 5G**). It is noteworthy that OCT4B overexpression had an even stronger moderating effect on EMT markers than OCT4-pg5 overexpression (**Fig. 5B-D**). Immunofluorescence staining also revealed markedly increased expression of E-cadherin and decreased expression levels of vimentin following OCT4-pg5 knockdown (**Fig. 5H-J**). These results demonstrated that OCT4-pg5 might promote BC metastasis by EMT, upregulating mesenchymal markers while downregulating epithelial marker.

OCT4-pg5 and OCT4B regulated EMT via a Wnt/β-catenin signaling pathway

The Wnt/β-catenin signaling pathway is implicated in the regulation of EMT, which in turn promotes metastasis (23). To examine potential contributions of Wnt/β-catenin signaling to EMT induction by OCT4-pg5 and OCT4B, we performed qRT-PCR, Western blotting, and immunofluorescence assays to measure changes in EMT signaling molecules in transfected T24 and 5637 cells. Downregulation of OCT4-pg5 and OCT4B reduced β-catenin expression, while OCT4-pg5 and OCT4B overexpression enhanced β-catenin expression (**Fig. 5E,F,G,K**).

OCT4-pg5 and OCT4B enhanced the resistance of T24 cells to cisplatin

Cisplatin is one of the first-line treatments for BC (24). We tested whether OCT4-pg5 or OCT4B could regulate the sensitivity of BC cells to cisplatin. Treated with 85 mmol/L cisplatin for 48h, transfection with si-OCT4-pg5 or si-OCT4B significantly downregulated OCT4-pg5 and OCT4B mRNA expression levels as measured by qRT-PCR (**Fig. 6A,B**), and the expression levels of both OCT4B mRNA and protein were reduced by OCT4-pg5 knockdown (**Fig. 6B,C**).

Flow cytometry showed that OCT4-pg5 or OCT4B downregulation increased cisplatin-induced apoptosis of T24 cells (**Fig. 6D**). Similarly, OCT4-pg5 downregulation increased the proportion of cisplatin-treated T24 cells in G1 phase and decreased the proportion in S phase (**Fig. 6E**). In addition, si-OCT4-pg5 and si-OCT4B co-transfection had a stronger effect on cisplatin-induced cell apoptosis and cell cycle regulation than si-OCT4-pg5 or si-OCT4B transfection separately (**Fig. 6E**). Mice injected with OCT4-pg5 or OCT4B or OCT4-pg5/OCT4B knockdown cisplatin-treated T24 cells developed significantly larger tumors than mice injected with untransfected T24 cells (control) **(Fig. 6F)**.

Discussion

Bladder cancer is characterized by extremely aggressive and high recurrence rate (25), and a poor prognosis happens to patients with high-grade tumors and once muscle invasion has occurred, the overall survival is even worse (26). Indeed, a deeper understanding of underlying molecular mechanisms is beneficial for BC patients. In this study, we demonstrated that miR-145-5p repressed the migration, invasion of BC cells, while OCT4B and OCT4-pg5 knockdown significantly decreased the BC cells proliferation, invasion, and increased the cell percentage of G1 phase, confirming that OCT4-pg5 and OCT4B exerted an oncogenic role in BC, while miR-145-5p inhibited the BC progression.

The competitive regulatory interactions among ncRNAs collectively constitute ceRNA networks that if dysfunctional, may disrupt the complex molecular circuitry maintaining appropriate levels of cell proliferation and phenotype stability, culminating in tumorigenesis and progression (27–29). Our study revealed that miR-145-5p can reduce the migratory and invasive capacities of BC cells in vitro, consistent with previous studies on other cancer cell types (30–32). Additionally, we found that the expression levels of OCT4-pg5 and OCT4B were upregulated in BC tissue samples and cell lines, and that OCT4-pg5 expression correlated with clinical and histopathological indices of prognosis, suggesting that OCT4-pg5 and OCT4B are oncogenic in BC as in other cancer types (12, 22, 33, 34).

Pseudogenes are implicated in the initiation and progression of cancers, at least in part by acting as microRNA decoys that disrupt normal miRNA-mediated regulation of oncogene (35). miR-145 can bind to OCT4 mRNA as well as to the OCT4 pseudogenes OCT4-pg1, 3, 4 and 5 (4), and previous report has demonstrated that OCT4-pg4 can regulate OCT4 expression and compete with miR-145-5p in hepatocellular carcinoma (36). Additionally, OCT4-pg5 acts as a miR-145-5p sponge in endometrial cancer, resulting in elevated OCT4 expression (22). Similarly, PTENP1 has been shown to function as a ceRNA that competes for miRNAs targeting the PTENP1 3'UTR (37), while miR-145-5p can regulate OCT4 expression by targeting the OCT4 3'UTR in various cancer types (38, 39). Given that the OCT4-pg5 3'UTR and OCT4B 3'UTR share the same miR-145-5p binding site and show the same free energy change upon binding, it appears that OCT4-pg5 competes equally with miR-145-5p for the OCT4B 3’UTR but does not trigger mRNA degradation. Indeed, inhibition of OCT4B expression by miR-145-5p could be reversed by OCT4-pg5 overexpression. Collectively, these results strongly suggest that OCT4-pg5 acts as an oncogene by functioning as a ceRNA, thereby elevating parental OCT4B expression.

In several cancer types, overexpression of OCT4B was reported to prevent apoptosis (11) and increase migration, invasion, and extracellular matrix degradation capacities by inducing various EMT-related genes (40). Further, several studies found that OCT4 upregulated the transcription factors N-cadherin and vimentin by activating β-catenin, while miR-145-5p inhibited EMT by blocking the expression of OCT4, thereby downregulating the expression of N-cadherin and vimentin (41–43). We also found that expressions of N-cadherin and vimentin were upregulated in BC cells by OCT4B overexpression as well as by OCT4-pg5 overexpression. However, OCT4B demonstrated stronger EMT induction potential than OCT4-pg5, suggesting that OCT4-pg5 may induce EMT indirectly by regulating OCT4B expression. The Wnt/β-catenin signaling pathway is known to promote metastasis by inducing EMT (23), and the LEF1/β-catenin-dependent WNT signaling pathway can be activated by OCT4 (44). Indeed, silencing β-catenin blocked Oct4/Nanog-mediated EMT (45). In the current study, β-catenin was activated by OCT4-pg5 and OCT4B, suggesting that OCT4-pg5 and OCT4B may induce EMT via Wnt/β-catenin signaling.

According to European Association of Urology (EAU) Guidelines, cisplatin-based chemotherapy remains the first choice for metastatic bladder cancer (MMIBC) (46). However, BC is still characterized by cisplatin-resistance through different molecular mechanisms (47). Studies have reported that OCT4 knockdown protected NSCLC cells from apoptosis and enhanced sensitivity to cisplatin treatment (48), while overexpression of OCT4 promoted the differentiation of lung cancer cells into SLCCs and increased

cisplatin resistance (49). Similarly in this study, OCT4-pg5 and OCT4B expression protected BC cells from cisplatin damage, while OCT4-pg5 knockdown increased cisplatin-induced apoptosis and reduced the proportion of G1 cells, possibly by disinhibiting OCT4 expression. Studies have demonstrated that the loss of pluripotency markers OCT4 was correlated with cisplatin-treatment resistance by affecting DNA damage response (DDR) (50). Therefore, further studies are needed to identify the biological mechanism linking N-cadherin and vimentin upregulation to OCT4-pg5/miR-145-5p /OCT4B axis activity and to confirm that this axis can regulate cisplatin sensitivity in BC cases, thereby altering disease progression and clinical outcome.

Conclusions

In conclusions, our study demonstrates that OCT4-pg5 can promote oncogenesis by competing with miR-145-5p for binding to OCT4B mRNA, thereby disrupting miR-145-5p -mediated OCT4B downregulation and leading to OCT4B overexpression, and ultimately greater BC cell proliferative and invasive capacity. These findings identify new potential therapeutic targets for BC.

List Of Abbreviations

BC
Bladder cancer
ceRNA
competing endogenous RNA
OCT4
Octamer-binding transcription factor 4
miR-145-5p
microRNA-145-5p
3’UTR
3’ untranslated region
EMT
Epithelial-to-mesenchymal transition
GDP
Gross Domestic Product
HIF
Hypoxia inducible factor
LncRNA
Long non-coding RNAs
TCGA
The Cancer Genome Atlas
BLCA
Bladder Urothelial Carcinoma

DERNAs
Differentially expressed RNAs
DElncRNAs
differentially expressed lncRNAs
DEmiRNAs
differentially expressed miRNAs
DEmRNAs
differentially expressed mRNAs
OS
Overall survival
NMIBC
Non-muscle-invasive bladder cancer
MIBC
Muscle-invasive bladder cancer

Declarations

Acknowledgements

We thank the patients and their families for the signed informed consent forms for clinical sample experiments. This study was supported by the Guangzhou Science and Technology Plan Project Basic and Applied Basic Research Project (202002030030), and the Guangdong Province Basic and Applied Basic Research Fund Project (2020A1515010044).

Funding

This study was supported by the Guangzhou Science and Technology Plan Project Basic and Applied Basic Research Project (202002030030), and the Guangdong Province Basic and Applied Basic Research Fund Project (2020A1515010044).

Ethical approval and consent to participate:

The study involving humans was approved by the Research Ethics Committee of General Hospital of Southern Theater Command, No. 2019-040. The procedures used in this study adhere to the tenets of the Declaration of Helsinki. All informed consent was obtained from the subjects and guardians.

The study involving animals was approved by the Institutional Animal Care and Use Committee of the General Hospital of Southern Theater Command, No. 2019025a. The methods used in this study adhere to the tenets of the Declaration of Helsinki, and are in accordance with ARRIVE guidelines for the reporting of animal experiments.

Conflict of interest: The authors declared no potential conflicts of interest.

Availability of data and material: The datasets generated and/or analysed during the current study are available in the TCGA-BLCA, NCBI and ensemble, [https://portal.gdc.cancer.gov/, https://www.ncbi.nlm.nih.gov/, and https://asia.ensembl.org/index.html].

Consent for publication: Not applicable

Authors' contributions: Wuer Zhou, Yue Yang, and Chenglin Yang: Writing- Reviewing and Editing, Wei Wang: Investigation, Conceptualization, Supervision, Zhi Cao, Xiaoyu Lin, Huifen Zhang, Yuansong Xiao and Xiaoming Zhang: Validation. All authors reviewed the manuscript.

References

1. Sung H, Ferlay J, Siegel RL, Laversanne M, Soerjomataram I, Jemal A, et al. Global Cancer Statistics 2020: GLOBOCAN Estimates of Incidence and Mortality Worldwide for 36 Cancers in 185 Countries. CA: a cancer journal for clinicians.2021;71(3), 209–249.
2. Teoh J Y, Huang J, Ko WY, Lok V, Choi P, Ng, CF, et al. Global Trends of Bladder Cancer Incidence and Mortality, and Their Associations with Tobacco Use and Gross Domestic Product Per Capita. European urology. 2020;78(6), 893–906.
3. Global Burden of Disease 2019 Cancer Collaboration, Kocarnik, J. M., Compton, K., Dean, F. E., Fu, W., Gaw, B. L., et al. Cancer Incidence, Mortality, Years of Life Lost, Years Lived With Disability, and Disability-Adjusted Life Years for 29 Cancer Groups From 2010 to 2019: A Systematic Analysis for the Global Burden of Disease Study 2019. JAMA oncology. 2022; 8(3), 420–444.
4. Patra S. K. Roles of OCT4 in pathways of embryonic development and cancer progression. Mechanisms of ageing and development. 2020;189, 111286.
5. Wang X, Zhao Y, Xiao Z, Chen B, Wei Z, Wang B, et al. Alternative translation of OCT4 by an internal ribosome entry site and its novel function in stress response. Stem cells (Dayton, Ohio).2009; 27(6), 1265–1275.
6. Chen S, Zhu J, Wang, F, Guan Z, Ge Y, Yang X, et al. LncRNAs and their role in cancer stem cells. Oncotarget.2017; 8(66), 110685–110692.
7. Lu CS, Shieh GS, Wang CT, Su BH, Su YC, Chen YC, et al. Chemotherapeutics-induced Oct4 expression contributes to drug resistance and tumor recurrence in bladder cancer. Oncotarget. 2017; 8(19), 30844–30858.
8. Iskender B, Izgi K, and Canatan H Reprogramming bladder cancer cells for studying cancer initiation and progression. Tumour biology: the journal of the International Society for Oncodevelopmental Biology and Medicine. 2016;37(10), 13237–13245.
9. Poursani EM, Mehravar M, Shahryari A, Mowla SJ, and Mohammad Soltani, B. Alternative Splicing Generates Different 5' UTRs in OCT4B Variants. Avicenna journal of medical biotechnology. 2017; 9(4), 201–204.

10. Lin SC, Chung CH, Chung CH, Kuo MH, Hsieh CH, Chiu YF, et al. OCT4B mediates hypoxia-induced cancer dissemination. Oncogene.2019; 38(7), 1093–1105.
11. Meng L, Hu H, Zhi H, Liu Y, Shi F, Zhang L, Zhou Y, et al. OCT4B regulates p53 and p16 pathway genes to prevent apoptosis of breast cancer cells. Oncology letters.2018; 16(1), 522–528.
12. Poursani EM, Mehravar M, Mohammad Soltani B, Mowla SJ, and Trosko JE. A Novel Variant of OCT4 Entitled OCT4B3 is Expressed in Human Bladder Cancer and Astrocytoma Cell Lines. Avicenna journal of medical biotechnology.2017; 9(3), 142–145.
13. Choi SH, Kim JK, Jeon HY, Eun K, and Kim H. OCT4B Isoform Promotes Anchorage-Independent Growth of Glioblastoma Cells. Molecules and cells.2019; 42(2), 135–142.
14. Xu WX, Liu Z, Deng F, Wang DD, Li XW, Tian T, Zhang J, et al. MiR-145: a potential biomarker of cancer migration and invasion. American journal of translational research.2019; 11(11), 6739–6753.
15. Chiyomaru T, Enokida H, Tatarano S, Kawahara K, Uchida Y, Nishiyama K, et al. miR-145 and miR-133a function as tumour suppressors and directly regulate FSCN1 expression in bladder cancer. British journal of cancer.2010; 102(5), 883–891. doi:10.1038/sj.bjc.6605570
16. Zhu J, Qin P, Cao C, Dai G, Xu L, Yang D. Use of miR145 and testicular nuclear receptor 4 inhibition to reduce chemoresistance to docetaxel in prostate cancer. Oncology reports.2021; 45(3), 963–974.
17. Chi Y, Wang D, Wang J, Yu W, Yang J. Long Non-Coding RNA in the Pathogenesis of Cancers. Cells.2019; 8(9), 1015.
18. Taheri, M., Omrani, M. D., Ghafouri-Fard, S. Long non-coding RNA expression in bladder cancer. Biophysical reviews.2018; 10(4), 1205–1213.
19. Hirotsune S, Yoshida N, Chen A, Garrett L, Sugiyama F, Takahashi S, et al. An expressed pseudogene regulates the messenger-RNA stability of its homologous coding gene. Nature.2003; 423(6935), 91–96.
20. Hu X. et al. Role of Pseudogenes in Tumorigenesis. Cancers (Basel).2018; 10.
21. Poursani EM, Mohammad Soltani B, Mowla SJ. Differential Expression of OCT4 Pseudogenes in Pluripotent and Tumor Cell Lines. Cell journal.2016; 18(1), 28–36.
22. Bai M, Yuan M, Liao H, Chen J, Xie B, Yan D, et al. OCT4 pseudogene 5 upregulates OCT4 expression to promote proliferation by competing with miR-145 in endometrial carcinoma. Oncology reports.2015; 33(4), 1745–1752.
23. Khan AQ, Ahmed EI, Elareer NR, Junejo K, Steinhoff M, Uddin S. Role of miRNA-Regulated Cancer Stem Cells in the Pathogenesis of Human Malignancies. Cells.2019; 8(8), 840.
24. Yoshida T, Kates M, Fujita K, Bivalacqua TJ, McConkey DJ. Predictive biomarkers for drug response in bladder cancer. International journal of urology: official journal of the Japanese Urological Association. 2019;26(11), 1044–1053.
25. Lenfant L, Aminsharifi A, Seisen T, Rouprêt M. Current status and future directions of the use of novel immunotherapeutic agents in bladder cancer. Current opinion in urology.2020; 30(3), 428–440.

26. D'Andrea D, Matin S, Black PC, Petros FG, Zargar H, Dinney CP, et al. Comparative effectiveness of neoadjuvant chemotherapy in bladder and upper urinary tract urothelial carcinoma. BJU international.2021; 127(5), 528–537.
27. Chan JJ, Tay Y. Noncoding RNA:RNA Regulatory Networks in Cancer. International journal of molecular sciences.2018; 19(5), 1310.
28. Anastasiadou E, Jacob LS, Slack FJ. Non-coding RNA networks in cancer. Nature reviews. Cancer.2018; 18(1), 5–18.
29. Mohapatra S, Pioppini C, Ozpolat B, Calin G A. Non-coding RNAs regulation of macrophage polarization in cancer. Molecular cancer.2021; 20(1), 24. doi:10.1186/s12943-021-01313-x
30. Li C, Xu N, Li YQ, Wang Y, Zhu ZT. Inhibition of SW620 human colon cancer cells by upregulating miRNA-145. World journal of gastroenterology.2016; 22(9), 2771–2778.
31. Azizmohammadi S, Safari A, Azizmohammadi S, Kaghazian M, Sadrkhanlo M, Yahaghi, E. Molecular identification of miR-145 and miR-9 expression level as prognostic biomarkers for early-stage cervical cancer detection. QJM: monthly journal of the Association of Physicians.2017; 110(1), 11–15.
32. Xu N, Papagiannakopoulos T, Pan G, Thomson JA, Kosik KS. MicroRNA-145 regulates OCT4, SOX2, and KLF4 and represses pluripotency in human embryonic stem cells. Cell.2009; 137(4), 647–658.
33. Choi SH, Kim JK, Jeon HY, Eun K, Kim H. OCT4B Isoform Promotes Anchorage-Independent Growth of Glioblastoma Cells. Molecules and cells.2019; 42(2), 135–142.
34. Soheili S. et al. Distinctive expression pattern of OCT4 variants in different types of breast cancer. Cancer Biomark.2017; 18, 69–76.
35. Lou W, Ding B, Fu P. Pseudogene-Derived lncRNAs and Their miRNA Sponging Mechanism in Human Cancer. Frontiers in cell and developmental biology.2020; 8, 85.
36. Wang L, Guo ZY, Zhang R, Xin B, Chen R, Zhao J, et al. Pseudogene OCT4-pg4 functions as a natural micro RNA sponge to regulate OCT4 expression by competing for miR-145 in hepatocellular carcinoma. Carcinogenesis.2013; 34(8), 1773–1781.
37. Poliseno L, Salmena L, Zhang J, Carver B, Haveman WJ, Pandolfi PP. A coding-independent function of gene and pseudogene mRNAs regulates tumour biology. Nature.2010; 465(7301), 1033–1038.
38. Matsushita R, Yoshino H, Enokida H, Goto Y, Miyamoto K, Yonemori M, et al. Regulation of UHRF1 by dual-strand tumor-suppressor microRNA-145 (miR-145-5p and miR-145-3p): Inhibition of bladder cancer cell aggressiveness. Oncotarget.2016; 7(19), 28460–28487.
39. Wu Y, Liu S, Xin H, Jiang J, Younglai E, Sun S, et al. Up-regulation of microRNA-145 promotes differentiation by repressing OCT4 in human endometrial adenocarcinoma cells. Cancer.2011; 117(17), 3989–3998.
40. Zhou JM, Hu SQ, Jiang H, Chen YL, Feng JH, Chen ZQ, et al. OCT4B1 Promoted EMT and Regulated the Self-Renewal of CSCs in CRC: Effects Associated with the Balance of miR-8064/PLK1. Molecular therapy oncolytics.2019; 15, 7–20.

41. Zhao H, Kang X, Xia X, Wo L, Gu X, Hu Y, et al. miR-145 suppresses breast cancer cell migration by targeting FSCN-1 and inhibiting epithelial-mesenchymal transition. American journal of translational research.2016; 8(7), 3106–3114.
42. Gao Y, Zhang Z, Li K, Gong L, Yang Q, Huang X, et al. Author Correction: Linc-DYNC2H1-4 promotes EMT and CSC phenotypes by acting as a sponge of miR-145 in pancreatic cancer cells. Cell death & disease.2019; 10(8), 604.
43. Li C, Lu L, Feng B, Zhang K, Han S, Hou D, et al. The lincRNA-ROR/miR-145 axis promotes invasion and metastasis in hepatocellular carcinoma via induction of epithelial-mesenchymal transition by targeting ZEB2. Scientific reports.2017; 7(1), 4637.
44. Sun L, Liu T, Zhang S, Guo K, Liu, Y. Oct4 induces EMT through LEF1/β-catenin dependent WNT signaling pathway in hepatocellular carcinoma. Oncology letters.2017; 13(4), 2599–2606.
45. Liu L, Zhu H, Liao Y, Wu W, Liu L, Liu L, et al. Inhibition of Wnt/β-catenin pathway reverses multi-drug resistance and EMT in Oct4+/Nanog + NSCLC cells. Biomedicine & pharmacotherapy = Biomedecine & pharmacotherapie.2020; 127, 110225.
46. Witjes JA, Bruins HM, Cathomas R, Compérat EM, Cowan NC, Gakis G, et al. European Association of Urology Guidelines on Muscle-invasive and Metastatic Bladder Cancer: Summary of the 2020 Guidelines. European urology.2021; 79(1), 82–104.
47. Drayton RM, Catto JW. Molecular mechanisms of cisplatin resistance in bladder cancer. Expert review of anticancer therapy.2012; 12(2), 271–281.
48. Liu X, Ma M, Duan X, Zhang H, Yang M, Knockdown of OCT4 may sensitize NSCLC cells to cisplatin. Clinical & translational oncology: official publication of the Federation of Spanish Oncology Societies and of the National Cancer Institute of Mexico.2017; 19(5), 587–592.
49. Chiou SH, Wang ML, Chou YT, Chen CJ, Hong CF, Hsieh WJ, et al. Coexpression of Oct4 and Nanog enhances malignancy in lung adenocarcinoma by inducing cancer stem cell-like properties and epithelial-mesenchymal transdifferentiation. Cancer research.2010; 70(24), 10433–10444.
50. de Vries G, Rosas-Plaza X, van Vugt M, Gietema JA, de Jong S, Testicular cancer: Determinants of cisplatin sensitivity and novel therapeutic opportunities. Cancer treatment reviews2020; 88, 102054.

Figures

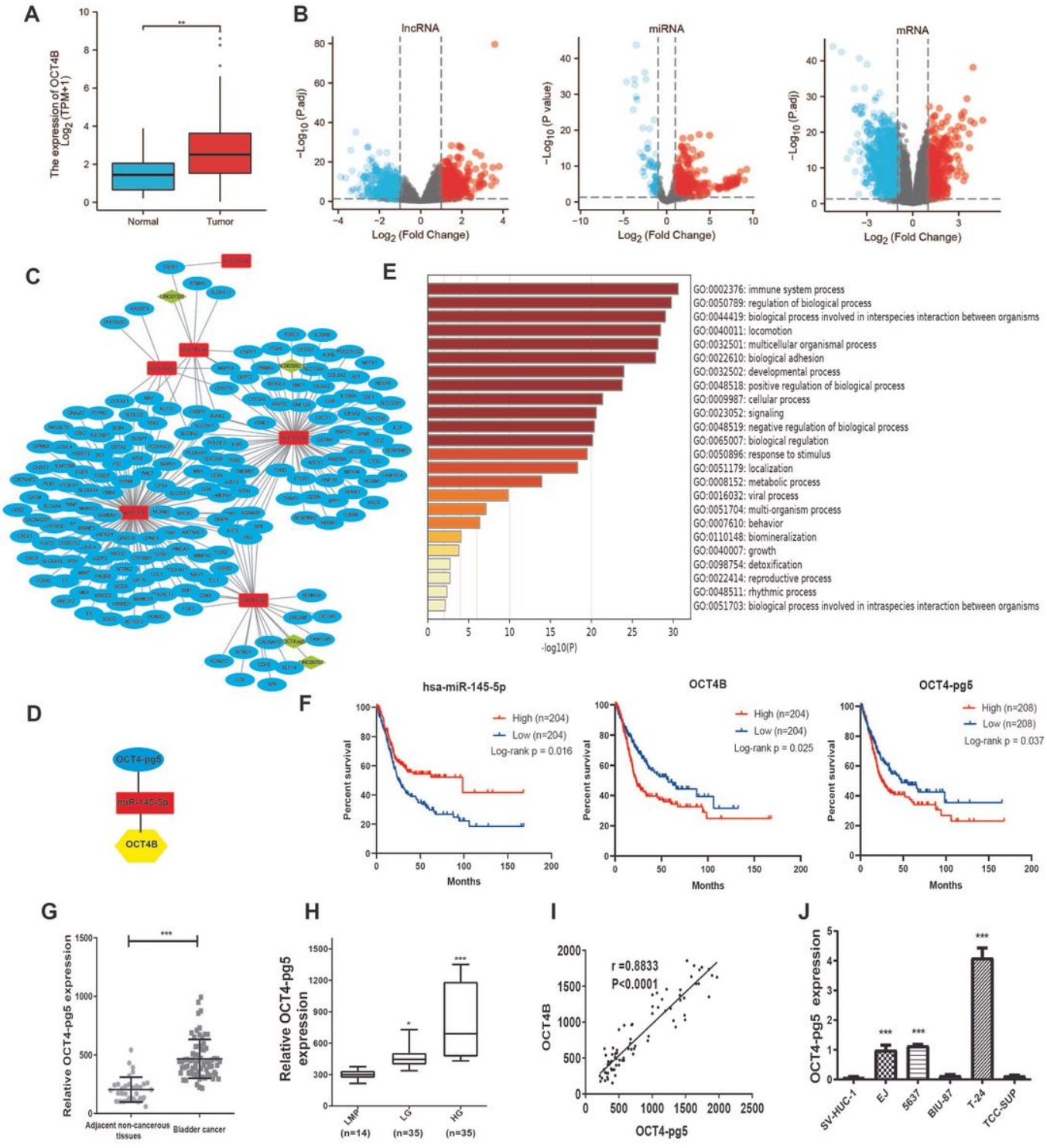

Figure 1

OCT4B is upregulated and associated with poor prognosis in bladder cancer (BC). **(A)** Expression distribution of OCT4B in TCGA BLCA cohort. **(B)** 133 DElncRNA, 175 DEmiRNAs, and 250 DEmRNAs. Red represents upregulated RNAs and blue indicates downregulated RNAs. **(C)** The triple regulatory network in the BC. Red indicates miRNAs, blue represents mRNAs, and green means lncRNAs. **(D)** Three hub RNAs in the network with a score of >2. **(E)** Functional enrichment analysis (GO and KEGG) of the DERNAs in the network. **(F)** The high and low expression values of three hub RNAs were compared by Kaplan-Meier

survival curves and log-rank test was used to analyze the overall survival rate for TCGA BLCA patient cohort. **(G)** OCT4-pg5 expression in BC tissues (n=140) and adjacent non-cancerous tissues(n=34). **(H)** OCT4-pg5 expression level in different histological grades of BC (Papillary urothelial neoplasms of low malignant potential, PUN-LMP; low grade, LG; high grade, HG). **(I)** Relationship between OCT4-pg5 and OCT4B mRNA expression levels in BC tissues. **(J)** All expression levels were measured by RT-PCR. OCT4-pg5 expression in different bladder cell lines (The expression levels were normalized to GAPDH expression). ***P < 0.001, *P < 0.05.

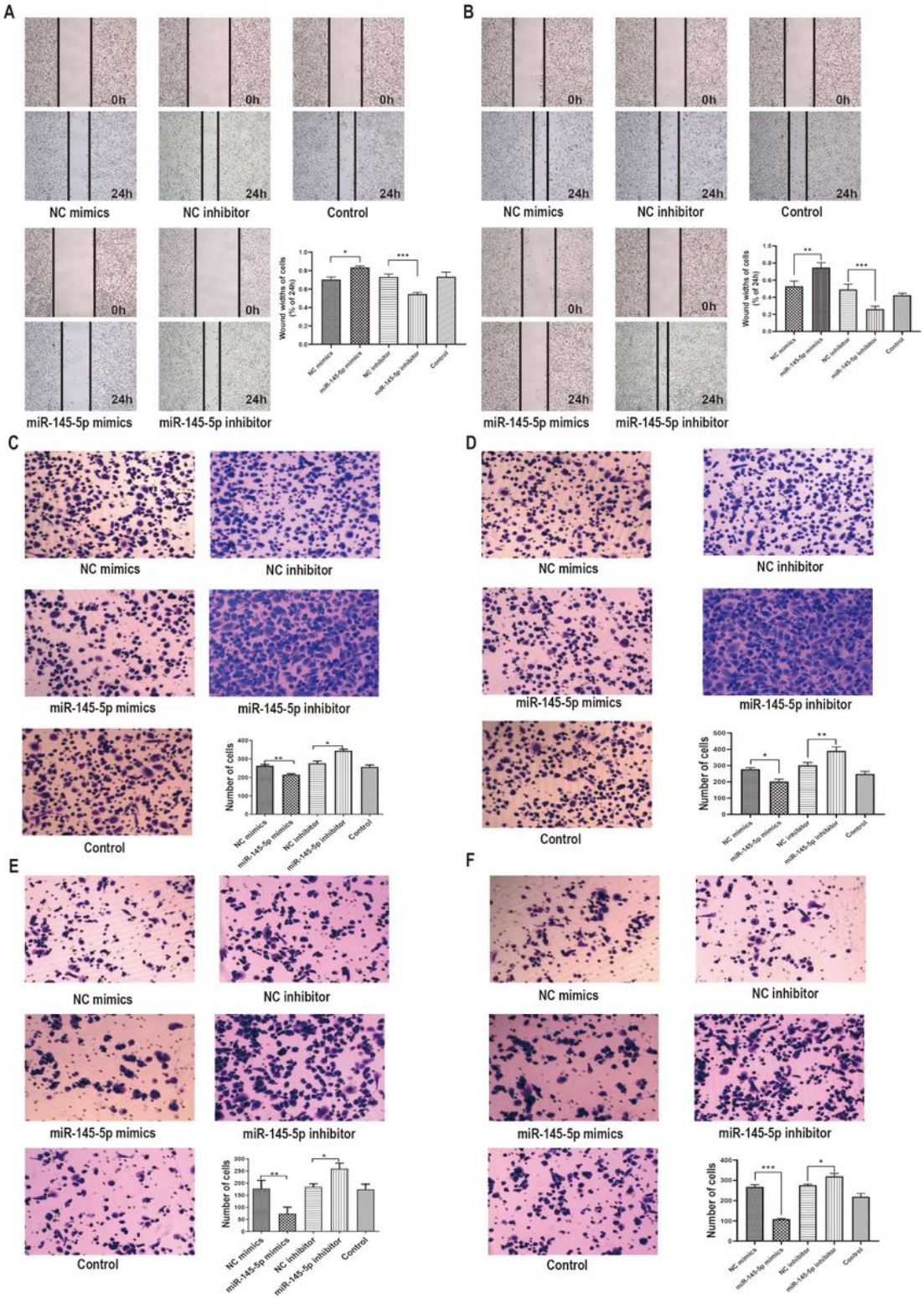

Figure 2

Overexpression of miR-145-5p reduces the migration and invasion potential of T24 and 5637 BC cells in vitro. **(A and B)** Effects of miR-145-5p on T24 and 5637 cell migrations as examined by wound healing assay (magnification, ×50). **(C-F)** transwell assays used to evaluate the effects of miR-145-5p on T24 and 5637 cell invasion **(C and D)** and migration **(E and F)**. Photographs of cell invasion and migration were acquired from polycarbonate membranes stained with crystal violet (magnification, ×200). (NC: negative control). ***P < 0.001, **P < 0.01, *P < 0.05.

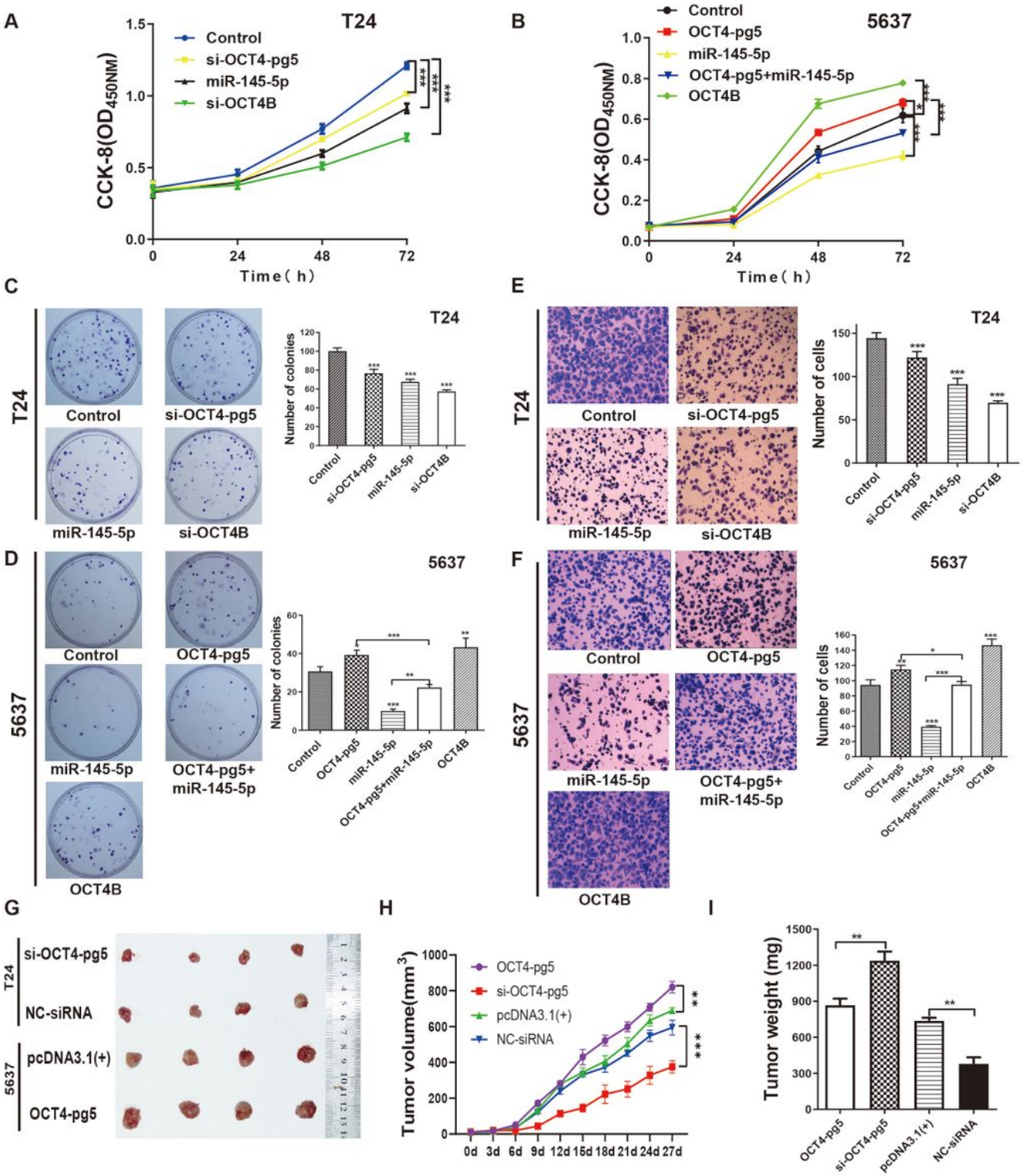

Figure 3

OCT4-pg5 and OCT4B function as oncogenes in BC cells in vitro and in vivo. **(A)** and **(B)** CCK-8 assays showing viable T24 and 5637 cell numbers at different times post-transfection with the indicated transcripts. **(C)** and **(D)** Colony formation assays to estimate the proliferation rates of T24 and 5637 BC cells. **(E)** and **(F)** Transwell assays to determine the invasion capacities of T24 and 5637 cells. **(G)** Tumor growth in vivo of the OCT4-pg5 silencing in T24 cells and OCT4-pg5 overexpression in 5637 cells. (NC-

siRNA: Negative control siRNA plasmid). **(H)** Tumor growth curves measured every three days after inoculation of T24 or 5637 cells. **(I)** Tumor weight was measured on the 27th day post-inoculation. ***P < 0.001, **P < 0.01, *P < 0.05.

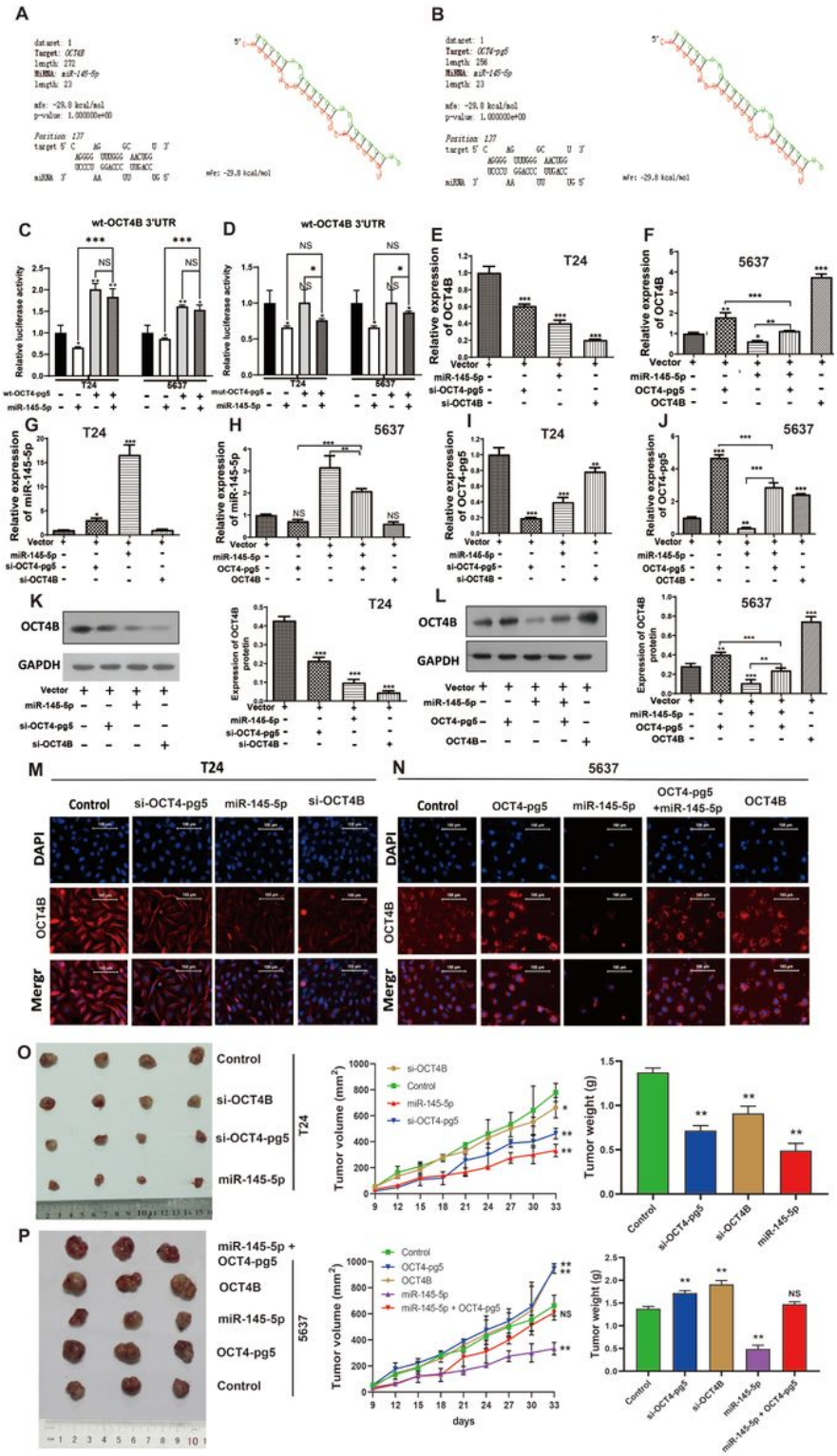

Figure 4

OCT4-pg5 3'UTR regulates the expression of OCT4B by sequestering miR-145-5p. **(A)** and **(B)** The binding force and possible secondary structure analyzed by RNAhybrid. **(C)** and **(D)** Luciferase activity of OCT4B reporters in T24 and 5637 BC cells. MiR-145-5p mimics, wild-type, or mutant OCT4-pg5 3'UTR were co-transfected with luciferase reporters. **(E-J)** Relative expression levels of OCT4B, miR-145-5p, and OCT4-pg5 in T24 and 5637 cells were measured by qRT-PCR (Normalized to GAPDH expression). **(K)** and **(L)** Relative expression levels of OCT4B protein in T24 cells and 5637 cells as measured by Western blot after the indicated transfection. Densitometric measures are shown to the right of each representative blot. **(M)** and **(N)** Immunofluorescence analysis of OCT4B expression in T24 cells and 5637 cells transfected with the indicated vectors. Red: Anti-OCT4B. Blue: DAPI nuclear staining. **(O)** and **(P)** Tumor growth curves measured every three days after inoculation of T24 or 5637 cells. ***P < 0.001, **P < 0.01, *P < 0.05.

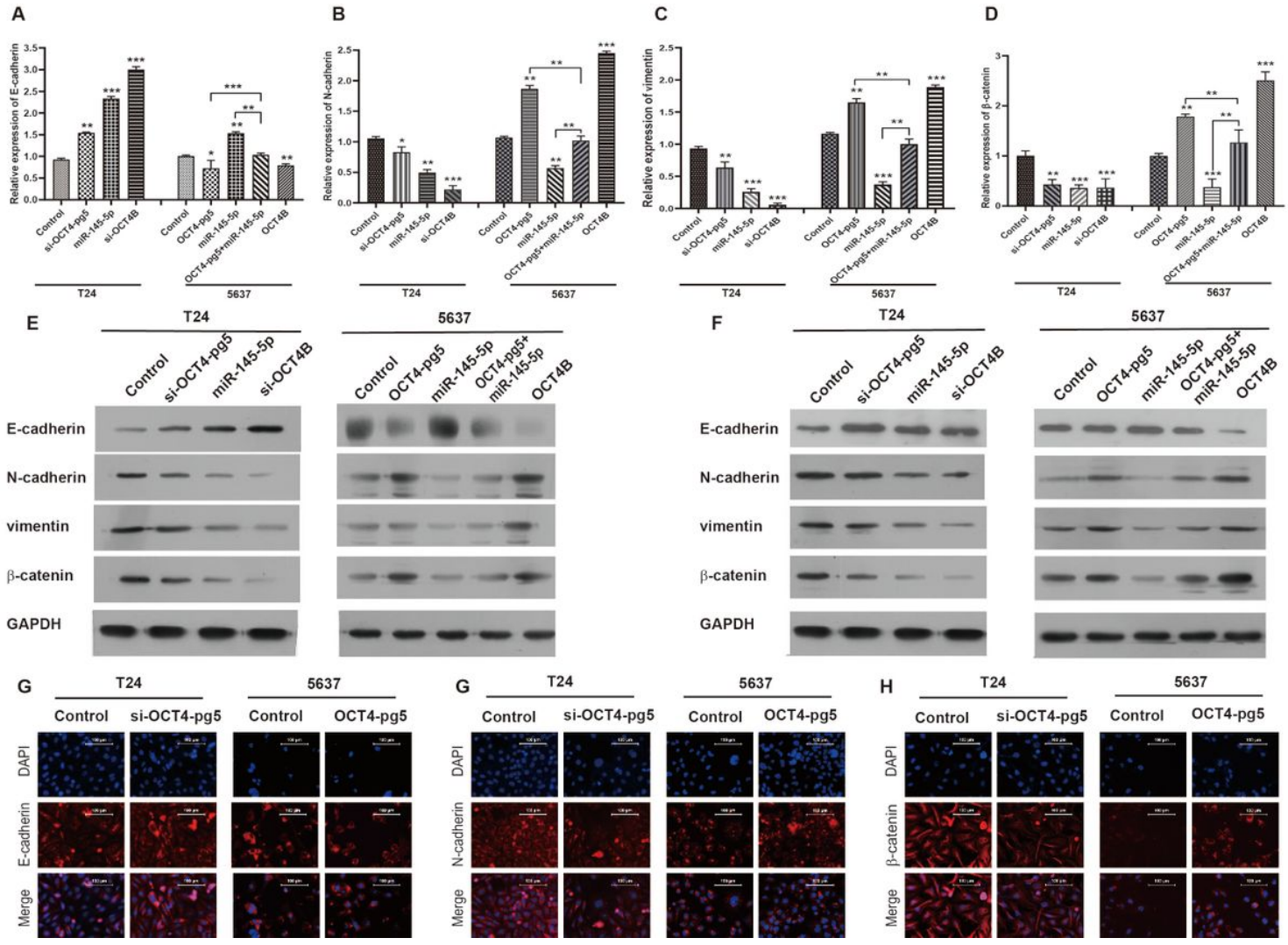

Figure 5

OCT4-pg5 promotes metastasis by inducing EMT through the Wnt/β-catenin pathway. **(A-E)** Relative mRNA expression levels of N-cadherin, vimentin, and E-cadherin in T24 cells and 5637 cells after transfection as measured by RT-PCR (normalized to GAPDH). **(F)** Relative protein expression levels of E-

cadherin, vimentin, and β-catenin in T24 cells and 5637 cells after transfection as measured by Western blot (normalized to GAPDH). **(G)** Relative protein expression levels of E-cadherin, N-cadherin, vimentin, and β-catenin in T24 cells and 5637 cells from nude mice as measured by Western blot (normalized to GAPDH). **(H-K)** Immunofluorescence staining for E-cadherin, vimentin, and β-catenin in T24 cells and 5637 cells. Red: anti-E-cadherin, anti-vimentin, and anti-β-catenin. Blue: DAPI nuclear staining. ***P < 0.001, **P < 0.01, *P < 0.05.

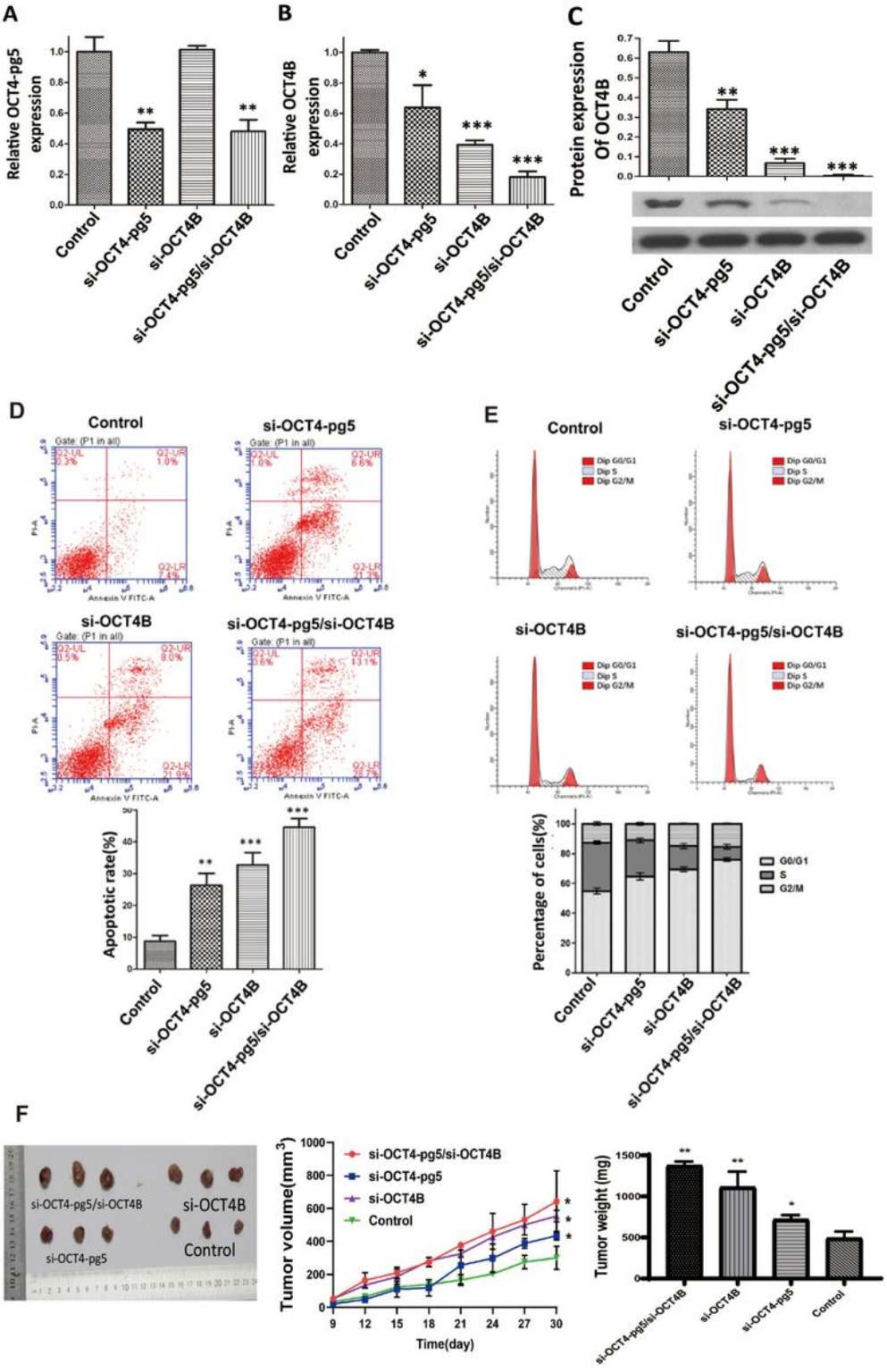

Figure 6

Crosstalk between OCT4-pg5 and OCT4B enhances the resistance of T24 cells to cisplatin. **(A)** and **(B)** OCT4-pg5 and OCT4B expression levels in T24 cells as measured by qRT-PCR. **(C)** Western blot analysis of OCT4B protein level in T24 cells. GAPDH was used as the control. **(D)** Effects of OCT4-pg5 3'UTR and OCT4B on the apoptotic rate of T24 cells as measured by flow cytometry. UL: necrotic cells, UR: terminal apoptotic cells, LR: early apoptotic cells, LL: normal cells. Cells in UR and LR were counted and analyzed. **(E)** Effects of OCT4-pg5 and OCT4B expression on the cell cycle stage distribution of T24 cells as measured by flow cytometry. **(F)** Tumor volume and weight was measured on the 27th day after injection with transfected T24 cells. ***P < 0.001, **P < 0.01, *P < 0.05.

Supplementary Files

This is a list of supplementary files associated with this preprint. Click to download.

- FigureS1.jpg
- FigureS2.jpg
- TableS1.docx
- TableS2.docx
- TableS3.docx
- TableS4.docx
- TableS5.docx
- TableS6.docx